MRI, CT, and PETSCAN: Engineer's Perspective

6

Subhankar Ghosh and Saurabh Pal

Abstract

We first discuss historical developments in tomographic imaging used for medical diagnosis. To discuss magnetic resonance imaging, we introduce the fundamental ideas of magnetic moment, nuclear magnetic moment, and total magnetization. Then, we clarify the notions on classical precession and the principle of magnetic resonance signal detection and explain spin–lattice and spin–spin relaxation. Further, the relevant details of MRI machine and its components like magnetic gradient coils, signal generation, and pulse sequence–*k*-space imaging are discussed in brief form.

We then introduce computed tomography (CT) based on X-rays. Basic concept of X-ray, different generations of CT, EBCT, helical CT, etc., are introduced. Various clinical applications of CT scan image are discussed in brief. The last item discussed is positron emission tomography scan (PET scan), its basic principle, and utilities. The concluding remarks regarding these imaging techniques and comparison in medical diagnosis are made.

Keywords

MRI · CT · PET scan · X-rays

S. Ghosh (✉)
Department of Physics, St. Xavier's College, Kolkata, India
e-mail: subhankar@sxccal.edu

S. Pal
Department of Applied Physics, University of Calcutta, Kolkata, India

S. K. Basu et al. (eds.), *Cancer Diagnostics and Therapeutics*,
https://doi.org/10.1007/978-981-16-4752-9_6

6.1 Introduction

This is a composite chapter discussing the underlying principles of three very important machines: magnetic resonance imaging, computed tomography, and positron emission tomography. These are widely used in complex medical diagnostics, especially for the detection of malignancies in different organs of human body. No medical center treating cancer can afford not to use the images produced by these machines. The presentation in this chapter is as follows. We first give historical developments in tomographic imaging in medical diagnosis. We then give introduction to magnetic resonance imaging, the machine.

Computed tomography (CT) is a widely adopted imaging technology, making the technology a reliable tool for noninvasive detection of unwanted growth and its progression in living bodies. This forms the second part of this chapter. Discussion is restricted to basic principle of computed tomography, development of CT scanning technology, and its clinical application.

Positron emission tomography (PET) is a very effective imaging technique used to explore the functionality of the different tissues and organs in the human body. This type of scan requires that a small amount of radioactive material (tracer) be delivered into the patient's bloodstream through intravenous injection. Once the tracer has spread through the body, the patient is taken to the scanning machine to have the procedure done.

This chapter is organized as follows: Sect. 6.2 deals with tomographic imaging in medical diagnosis, Sects. 6.3 and 6.4 deal with MRI, Sects. 6.5 through 6.10 deal with CT, Sects. 6.11 and 6.12 deal with PETSCAN, and Sect. 6.13 concludes the chapter.

6.2 Tomographic Imaging in Medical Diagnosis: Historical Developments

Whenever light (an electromagnetic wave) falls on any object, it gets reflected or refracted with part absorption in general. Both the reflection and the refraction help in the formation of an image. The image is sometimes real (can be seen on a screen) or virtual at times. This image formation and detection by eyes are daily experience for all of us. But when a small object is to be seen, we like the magnified view. This magnification was achieved historically by using lenses, mirrors, and other optical instruments. The simple microscope was an important beginning in this regard and seen as of paramount importance in medical diagnosis. Subsequent improvement in the form of compound microscope helped in the detection of disease-causing agents and many physiological studies.

In the twentieth century, mankind was gifted with two important discoveries in physics: the invention of X-ray by German Physicist Wilhelm Conrad Röntgen and the discovery of the electron by British Physicist J. J. Thomson. X-ray could be used to directly image the human body parts like bones. On the other side, limitation of the magnification ($\leq$1000 X) for the optical microscope was overcome by using

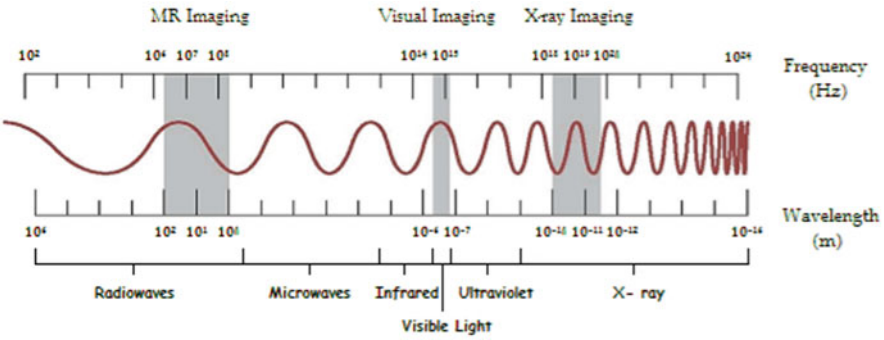

Fig. 6.1 Different ranges of the electromagnetic spectrum used for various imaging systems

electrons as beam in the revolutionary imaging technique known as electron microscope. Throughout the last few decades, the imaging techniques gradually matured in terms of precision, resolution, portability, and affordability in perfect harmony with the progress through inventions in the broad fields of biology, chemistry, and physics.

It is well known that the electromagnetic energy is a result of two mutually perpendicular fields, namely electric and magnetic fields that travel together in free space with the speed of light (~1,86,000 miles per second or 3,00,000 kilometers per second). As different amounts of electromagnetic energy are associated with the different ranges of the electromagnetic spectrum, most imaging techniques fall at different ranges of the electromagnetic spectrum depicted by Fig. 6.1.

As the history says, the X-ray, ultrasonography (USG), and nuclear medicine diagnostic tools supplement the sophisticated ones like magnetic resonance imaging (MRI), computed tomography (CT), positron emission tomography (PET SCAN). Some of the later techniques carry the common term as "Tomography," which is a combination of the Greek word *"tomos"* that means slice or section and English word *"graphy"* that means technique.

In this chapter, we discuss the basic principles behind the three important imaging techniques (MRI, CT, and PET scan) and how MRI, CT, and PETSCAN help in detecting cancer cells. Also, another point needs special mention here. We have restricted the basic principles to classical mechanics and physics although the fundamental ideas like the magnetic moment of proton and its behavior in an external magnetic field (MRI), the annihilation of electron–positron pair, and resulting photons (PET) are quantum phenomena and demand familiarity in the area of quantum mechanics. But there is no harm in projecting classical analogies for the above-mentioned imaging techniques.

6.3 Magnetic Resonance Imaging (MRI)

The principal components of an MRI process (Liang and Lauterbur 2000; Brown and Semelka 2003) are the following steps: It stimulates a signal from the object or the patient body parts using both the magnetic field and the radiofrequency pulse. It then reads the experimental data using magnetic gradients and puts it into *k*-space related to the frequency domain. Thereafter, the frequency domain data get transformed into spatial domain that helps in resulting in an observable image.

6.3.1 The Machine: A Gigantic Chamber

An MRI machine consists of primarily the following parts: the magnet, the radiofrequency coils, the gradient coils, and the imaging accessories as shown in Fig. 6.2.

The magnet is the heart of a MRI scanner controlling the image quality and the cost decision. Magnetic field is measured in terms of two popular units: tesla (T) as the SI unit and gauss (G) as the C.G.S unit (1 tesla = 10 kilogauss). The earth's magnetic field is of the order of 0.6 T. There are normally three types of magnet that can be used here: permanent (up to 0.4 T), resistive (up to 0.6 T) using coils with current and superconducting (0.5–3 T—clinical limit) using superconducting coils with cryogens (to maintain very low temperature). Superconducting magnets are the common one with the five important aspects of field strength, homogeneity, shimming, sitting ease, and cryogen consumption.

The patient has to lie by being as still as possible on the table that enters through the chamber assembly. Now to appreciate the MRI process in totality, we digress a bit for firstly understanding the MRI signal followed by the concepts over the magnetization vector and pinpointing the signal using magnetization gradient and

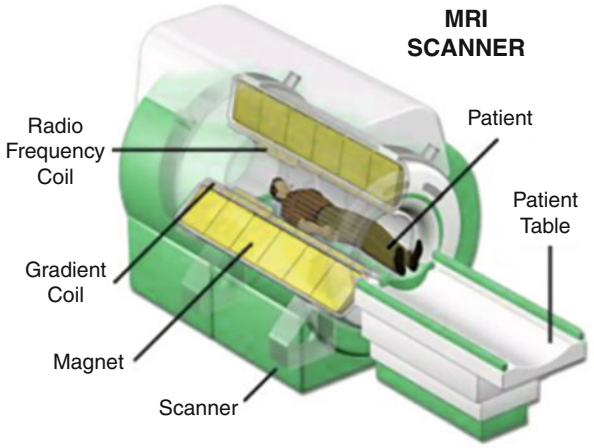

Fig. 6.2 MRI machine diagram

creating suitable signal, and finally the pulse sequence and collecting the emitted signal with the idea on *K*-space.

6.3.2 Magnetic Moment

It is now well known that the atom of any element is composed of fundamental particles like negatively charged light particle "electron," positively charged heavy particle "proton," and electrically neutral but heavy particle "neutron." A charged particle gives rise to an electrostatic or electric field. But if it moves with an acceleration or rotates with a frequency, the same particle generates a magnetic field. Thus, an electron possesses an angular momentum as it revolves around the central tiny nucleus (protons and neutrons) and a magnetic moment also.

A bar magnet (Fig. 6.3) is made up of two poles: north and south at the ends (strictly speaking, located inside at approximately 0.83 of its geometric length).

The magnetic moment ($\boldsymbol{M}$) is the product of magnetic pole strength (m) and the length ($\boldsymbol{l}$) or separation of the poles; that is, $\boldsymbol{M} = m \times \boldsymbol{l}$. The bar magnet experiences a *torque or turning moment* in an external magnetic field $\boldsymbol{B}$ and is expressed as $\boldsymbol{\tau} = \boldsymbol{M} \times \boldsymbol{B}$.

The electron also spins about its own axis like a top (modern idea about spin based on quantum mechanics does not require this similarity: Spin is an intrinsic property of particles like charge and mass). Thus, the electron acquires a spin-based angular momentum and the corresponding magnetic moment also. They are related by a simple relation $\boldsymbol{\mu}$ **or** $\boldsymbol{M} = (e/2\,m)\,\boldsymbol{L} = \boldsymbol{\gamma}\,\boldsymbol{L}$, where e is the electron charge, m is the mass of the electron, and $\boldsymbol{L}$ is the angular momentum. The factor of $\boldsymbol{\gamma} = (e/2\,m)$ is known as *gyromagnetic ratio* (sometimes called as magnetogyric ratio) for the electron. The $\boldsymbol{\gamma}$ value for the electron is 1.76×10^8 MHz / T (megahertz per tesla).

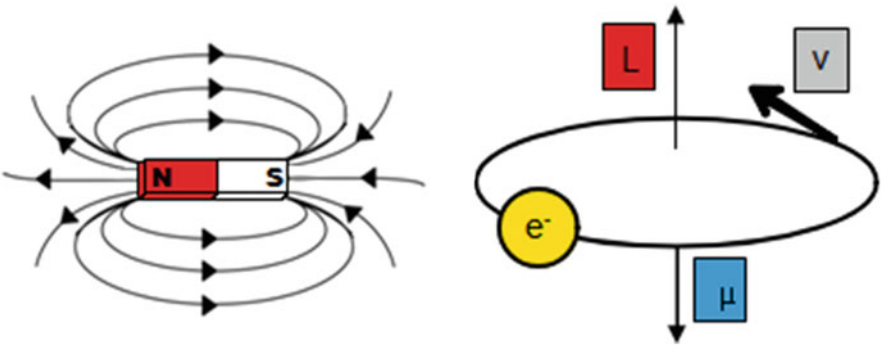

Fig. 6.3 Lines of force of a bar magnet and electron as a magnet

6.3.3 Nuclear Magnetic Moment

From the basics of atomic structure, we know that an atom of every element contains a tiny nucleus with positive charge at the core surrounded by the electrons, which revolve in different orbits. The nucleus consists of mainly two types of particles—positively charged protons and neutral neutrons. A proton is considered as a charged particle spinning around an internal axis of rotation with certain angular momentum and also a magnetic moment for which it can be treated as a very tiny bar magnet (see Fig. 6.4).

Unlike the electron, the magnetic field or magnetic moment due to the spin of the proton coincides with the sense and direction of the angular momentum on the spin axis. The proton magnetic moment is given by $\boldsymbol{\mu} = \boldsymbol{\gamma} \boldsymbol{L}$. The gyromagnetic ratio ($\boldsymbol{\gamma}$) has a value of 42.575 MHz / T. Thus, the sensitivity of detection in magnetic resonance is determined by the strength of the magnetic moment, which varies for different types of nucleus. Hydrogen is the first element in the modern periodic table, and its nucleus contains a single proton and, consequently, the highest magnetic moment. Further, it is found abundantly in organic tissues or matters. It is therefore the best choice as the nucleus used in the MRI process.

When there is no external magnetic field, as shown in Fig. 6.5, the magnitude of the magnetic moment of every proton (the hydrogen nucleus) is fixed in our body and their orientations are completely random. Therefore, the net magnetization or the vector sum of all the individual magnetic moments in human body is zero. However, when we apply a static magnetic field and electromagnetic radiation, the spin angular momentum of the hydrogen atoms interacts and produces a finite magnetization.

With the external constant magnetic field ($\mathbf{B_0}$) applied, the magnetic moment now can have only two possible discrete values in the direction of $\boldsymbol{B_0}$ following the principles of quantum mechanics. Therefore, it results in the magnetic moments being aligned at an angle of $\theta = 54.7^\circ$ with respect to B_0, either in the same favorable direction or in the opposite direction (Fig. 6.5). The first configuration is known as the parallel and the latter as the antiparallel configuration for the magnetic moments.

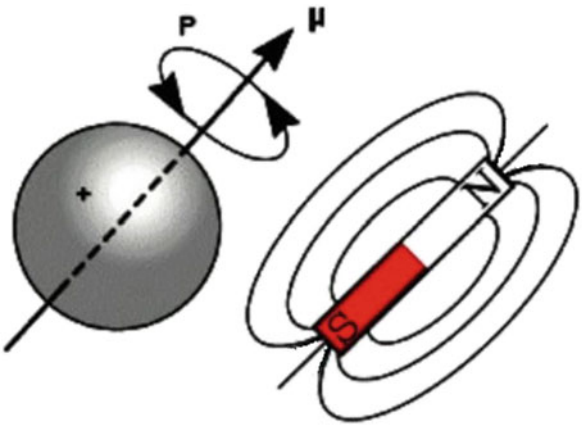

Fig. 6.4 Proton or nucleus behaves like a bar magnet

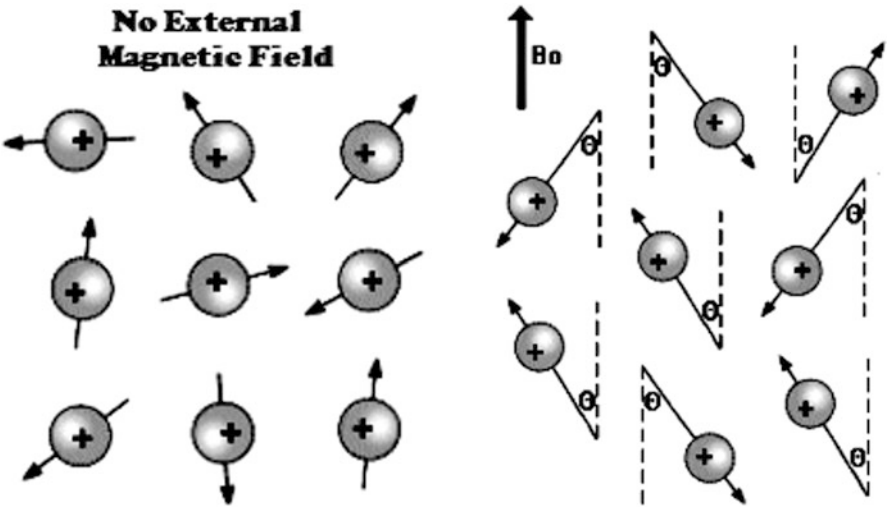

Fig. 6.5 Orientation of the proton magnetic moments

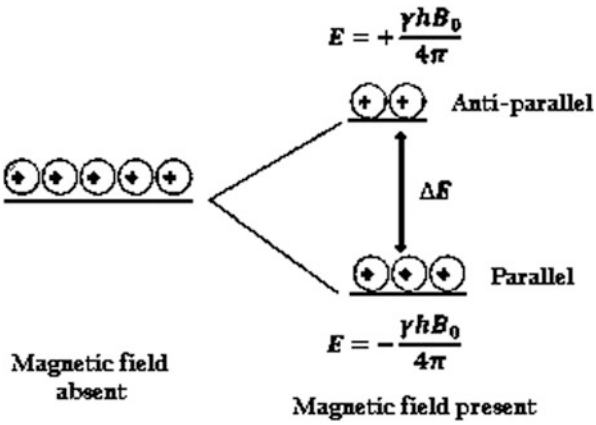

Fig. 6.6 Proton configurations (*left*: no magnetic field; *right*: Strong magnetic field is present)

It is found that the relative number of hydrogen protons in the parallel and antiparallel configurations depends upon the value of external constant magnetic field. Quantum mechanical calculations show that the protons in the parallel configuration have a lower energy state in comparison with those in the antiparallel state. Thus, in the absence of the external magnetic field, the protons have the same energy because of their random orientations. But with a strong magnetic field, the single energy level gets split into two energy levels depending on their parallel or antiparallel states. Here, the energy difference between the two energy states depends on the value of the external constant magnetic field. The energy difference (ΔE) between the above two energy states is shown in Fig. 6.6. It is important to note that only the difference

between the number of parallel and antiparallel and not the total number of protons is the guiding factor in the principle of the MRI process.

At any finite temperature, the two orientations of parallel or antiparallel are almost equally populated. So, the thermal energy fluctuations minimize the energy difference (ΔE) and result in a net bulk magnetization vector $\boldsymbol{M}$. Thereafter, with the electromagnetic radiation present, the protons can absorb or emit photons with an energy equal to ΔE and change its orientation.

6.3.4 Classical Precession

The motion of the proton magnetic moments can most easily be described using classical mechanics. The external magnetic field $\boldsymbol{B}_0$ attempts to align the proton magnetic moment with itself, and this action creates a torque ($\boldsymbol{C}$) given by the vector cross-product of the magnetic moment ($\boldsymbol{P}$) and the magnetic field $\boldsymbol{B_0}$ that means $\boldsymbol{C} = \boldsymbol{P} \times \boldsymbol{B_0}$.

As shown in Fig. 6.7, the external constant magnetic field $\mathbf{B}_0$ influences motion of the proton to result in precession around the axis of the magnetic field being inclined at a constant angle of $\theta = 54.7°$. Here, the torque that is defined as the rate of change in the angular momentum is responsible for the proton to precess around $\mathbf{B}_0$ at a frequency $\boldsymbol{\omega_L}$ known as Larmor frequency. This frequency termed is named after renowned Irish physicist Joseph Larmor. It is directly proportional to the strength of the magnetic field, i.e., $\boldsymbol{\omega_L = \gamma B_0}$.

For the hydrogen atom, the value of γ is 42.575 MHz / T. For a 1.0 T MRI machine, the Larmor frequency for hydrogen is 42.575 MHz. With a smaller magnetic field of 0.5 T, the Larmor frequency for hydrogen is approximately equal to 21.29 MHz. But For a 1.5 T MRI scanner, it becomes equal to 42.575 MHz / $T \times 1.5\ T = 63.86$ MHz. In comparison, the 3.0 T MRI scanner has the Larmor

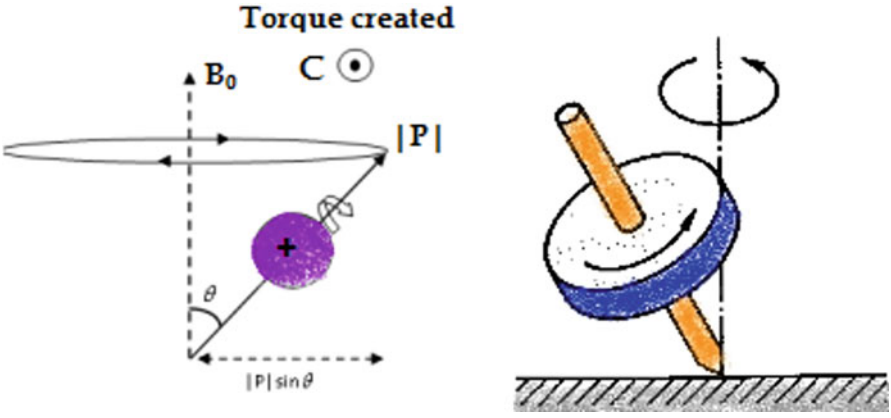

Fig. 6.7 (*Left*) A proton spinning about an internal axis is also precessing about the vertical axis (the direction of $\boldsymbol{B}_0$); (*Right*) Classical precession of a spinning top

frequency of 127.72 MHz. So, it is clear that the magnetic field strength and the Larmor frequency are directly proportional to each other. One can observe that the magnetic resonance frequencies are close to the radiofrequency range (RF range) of the electromagnetic energy spectrum.

6.3.5 Total Magnetization

The net magnetization can be calculated by the superimposition of several proton magnetic moments in a simple vector form. The vector sum of the components in a Cartesian coordinate system has only a vertical or z-component as in Fig. 6.8, while the vector sum of the components on the x- and y-axes is zero. It is therefore clear that the net magnetization has only a z-component nonvanishing.

6.3.6 Radiofrequency Pulse: Related Magnetization

An NMR signal in a MRI scanner is normally detected through a condition known as resonance condition. To understand resonance in our day-to-day world, we can consider the case of mechanically vibrating systems. The resonance condition is basically a state of alternating absorption and dissipation of energy. The stretched wire on a guitar can be plucked at any point to set up transverse vibration, but the sound may not be loud enough to be heard. A hollow wooden box with a hole beneath the striking point of the guitar string provides a resonating system to boost the intensity of the sound. It can be analytically shown that if the frequency of the forcing vibration is the same as the natural frequency of the body, then resonance

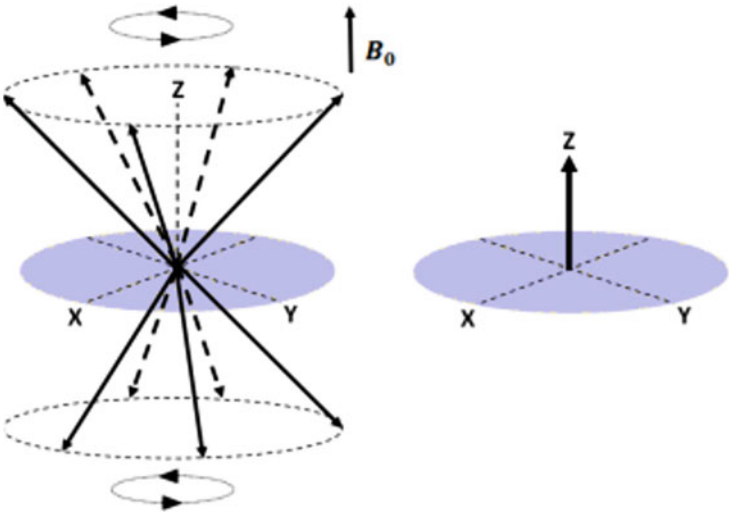

Fig. 6.8 (*Left*) Individual magnetization vectors and (*right*) their vector sum

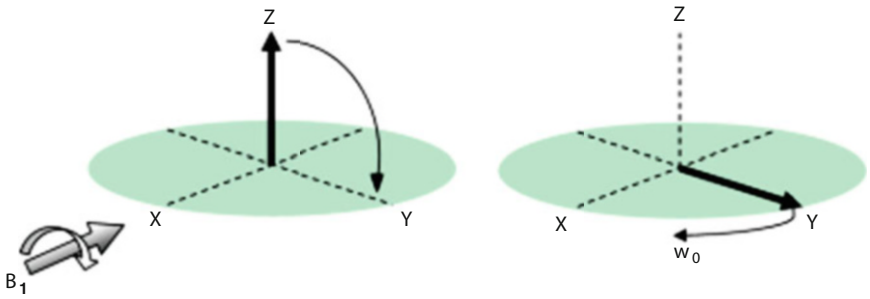

Fig. 6.9 (*Left*) RF pulse applied and (*right*) RF pulse is switched off

with large amplitude takes place. The same is the case of electrical resonance circuit. If the frequency of an alternating voltage/current source is the same as the natural frequency of a LCR (impedance, capacitor, resistor) circuit, current resonance can take place.

Here, in the MRI machine, the energy is supplied as a radiofrequency (RF) field with a certain frequency. When a RF pulse is applied, energy is absorbed and it gets dissipated through the relaxation processes. The energy levels for hydrogen atoms or protons in a magnetic field are similar to the multilevel energy values in a semiconductor. The generation of a MR signal requires an energy necessary to stimulate transitions between the energy levels. It can be seen that the frequency of the RF field is the same as the precession frequency or Larmor frequency. Let us now consider the application of a RF radiation with Larmor frequency to a nonmagnetic material in the presence of an already existing static magnetic field. The magnetic field component associated with the RF pulses is denoted by B1, which lies in a plane normal to B_0, as shown in Fig. 6.9. If we follow the same classical treatment of the proton precession, the new magnetic field $B1$ creates a torque on the proton. This causes the net magnetization vector M to rotate through a certain angle away from the B_0 axis toward the X-Y plane as shown in Fig. 6.9. This angle of rotation is known as the i_p angle. This angle is directly proportional to both the applied RF field intensity and the time of duration of $B1$. One can now easily guess the basic point: If the RF field component $B1$ lasts for a proper duration, the magnetization vector M can be made to rotate onto the transverse plane. That means, while in the transverse plane and rotating with the Larmor frequency, M will induce an NMR signal in the RF receiver coil placed in the transverse plane as shown in Fig. 5.9. This signal helps to observe the characteristics of M in the transverse plane and constitute the basis of MR signal detection. The nomenclature that follows is such the radiofrequency field that brings the magnetization vector M into the transverse plane is known as the 90° pulse. Further, an i_p angle of 90° results in maximizing the M_y component of magnetization. In contrast, a pulse of 180° produces no M_y magnetization but rotates the net magnetization M_0 from +z- to the -z-axis. The i_p angle of 90° is very important as it produces the strongest NMR signal with the magnetization vector M rotating in the transverse plane. But, the i_p angle of 180° is primarily important when applied in the

spin-echo imaging technique. Here, the reversal of the direction of M is made when it is on the transverse plane.

6.4 MR Signal Detection

Generally, the MRI detector is made up of a pair of conductive loops like copper wires that are mutually perpendicular to each other and are placed close to the subject (patient). From the basics of electromagnetic induction principles (Faraday's law), one can understand the development of a voltage (V) induced in each of these loops. The voltage has a value that is directly proportional to the rate of change in the magnetic flux (magnetic field intensity multiplied by the area) with time. Figure 6.10 shows magnetization vector M (precessing in the XY-plane) producing a voltage or the MR signal. It is obvious that the vertical or z-component of magnetization M does not precess, and hence, it is not effective in the generation of any voltage or signal.

6.4.1 MR Signal Intensity

The intensity of the MR signal received is determined by the following factors.

- It is proportional to the number of hydrogen atoms or protons in the subject. Thus, it is representative of the number of protons in each voxel of the image.
- As the value of magnetization M_0 is proportional to the external magnetic field B_0, a 2 tesla MRI system has twice the M_0 of a 1 tesla system.
- Further, the induced voltage is directly proportional to the precession frequency or to $B_{0,}$ and consequently, the MR signal is proportional to the square of the B_0 field. That is why the scientists are putting more efforts toward MRI systems with higher fields applied.

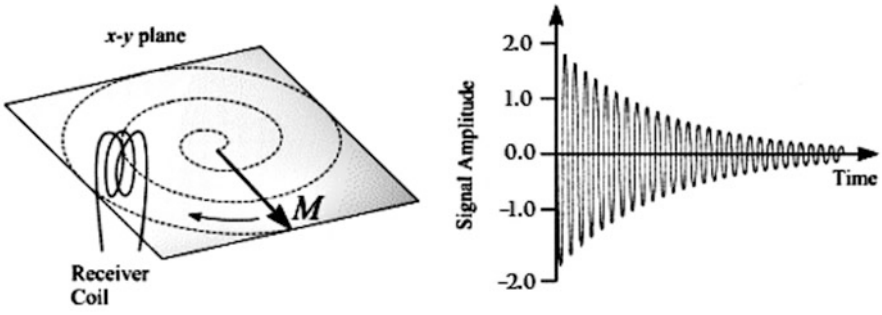

Fig. 6.10 MR signal produced through the effect of electromagnetic induction

6.4.2 Relaxation: Spin–Lattice (*T*1) and Spin–Spin (*T*2)

Now, let us try to understand the relaxation process as conceived in the MRI machines. In the presence of a strong constant magnetic field B_0, the equilibrium magnetization state corresponds to a z-component (M_z) equal to M_0 and both the transverse components of M_x and M_y being equal to zero (Fig. 6.11). As the RF pulse with a suitable frequency is applied, it adds energy to the whole system and, consequently, results in a nonequilibrium state. As soon as the pulse gets switched off, the system relaxes back to the thermal equilibrium state. Relaxation is a common term in many of the excitation phenomena in the physical processes. If we consider an active electrical circuit containing a combination of resistance and capacitance (RC) or resistance and inductance (RL) and apply an impulse voltage pulse across to any of them, the circuit develops time-varying voltages across each of the resistance, inductance, and capacitance. After a certain time span usually signified by the time constants, these time-varying voltages get back to their previous values before the application of the pulse. Similarly, with the application of a 90° RF pulse, the magnetization vector M rotates in the transverse plane with the Larmor frequency. It then decays to zero gradually as shown in Fig. 6.10.

Two different relaxation times generally govern the return of the z-component and the x- and y-components to their equilibrium values. Firstly, the $T1$-relaxation mechanism controls only z-component of the magnetization vector M and is also known as the spin–lattice relaxation. Secondly, the $T2$ relaxation affects only x- and y-components of magnetization and is referred to as the spin–spin relaxation. It thus governs the return of the M_x and M_y components of magnetization to their thermal equilibrium values of zero. Mathematically, the MR relaxation process is analyzed by applying the first-order differential equations (Bloch equations) and their solutions show how the M_z component changes with the i_p angle of an RF pulse at a time t after the application. It has been found that different tissues in human and other bodies have different values of $T1$ relaxation time. But the $T1$ relaxation time gets significantly changed for the dead or diseased tissues. Needless to say is that the

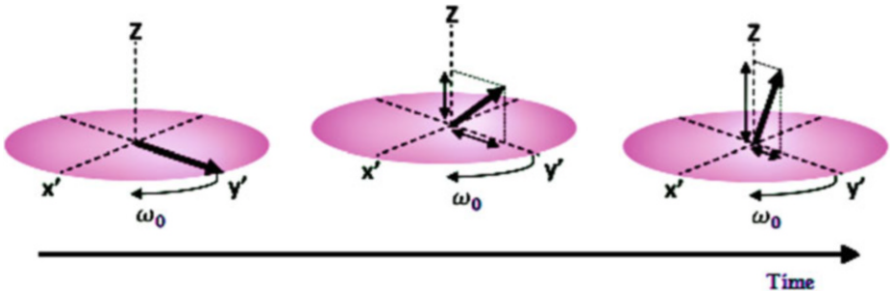

Fig. 6.11 (Left) Orientation of the magnetization vector after a 90° RF pulse is applied about the x-axis. (Center) $T1$ and $T2$ relaxation of the magnetization results in an increased M_z component and reduced M_y component, respectively, at a certain time after the pulse has been applied. (Right) The values of M_z and M_y components become M_0 and zero, respectively, at a later time

resulting differences are the basis for introducing contrast into the MR image. Again, for the second relaxation time $T2$, similar observations of different values for different tissues like healthy and dead or deceased in the body are used to differentiate between them in the final clinical images available.

6.4.3 Magnetic Gradient Coils

To translate the theoretical basis of magnetic resonance (MR) into a powerful imaging technique requires the use of magnetic gradient coils. The idea is based on the central understanding that if the applied magnetic field varies spatially within the body, it results in a spatial variation of the resonant frequencies, which, in turn, can help us in producing an image of high quality. Further, as the spatial variations have to be made dynamically, three separate "gradient coils" are incorporated into the experimental design of an MRI scanner. It is an engineering marvel that these gradient coils are designed as linear to ensure that the magnetic field varies linearly with respect to spatial location.

The gradient coils need to be fabricated such that there is no extra contribution to the magnetic field at the center of the Cartesian coordinate system ($z = 0$, $y = 0$, $x = 0$), also known as isocenter of the gradients. Thus, the magnetic field there is just equal to B_0 (Fig. 6.12). Then, the three separate magnetic field gradients are produced by passing a high value of direct current through separate coils with the help of high-power gradient amplifier and can be turned on and off very quickly with computer control. Conventionally, the y-axis points to the anterior/posterior direction and the x-axis corresponds to the left/right direction of the patient as shown in Fig. 6.13.

Three types of field gradients (Fig. 6.14) are generally used in an MRI scanner namely slice selection along the z-axis, phase encoding along the x-axis, and frequency encoding along y-axis. The amplitude and duration of these field gradients are critically important in reading the information in k-space. Points in k-space are generated by manipulating these gradients.

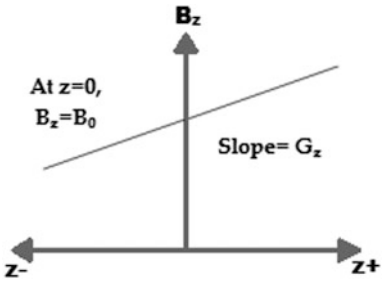

Fig. 6.12 The resulting magnetic field B_z as a function of the z-direction

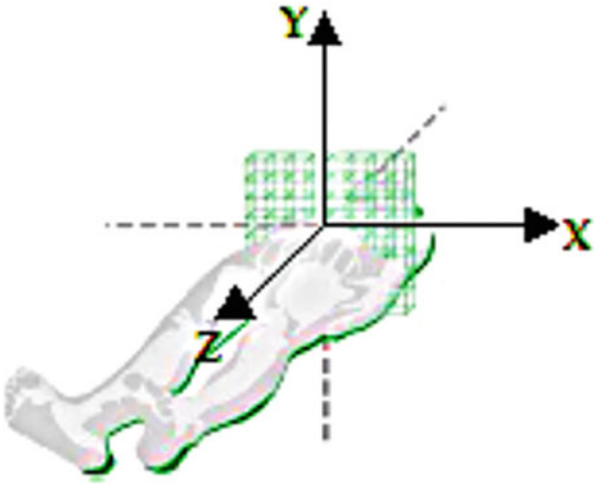

Fig. 6.13 Different axes for the gradient coil

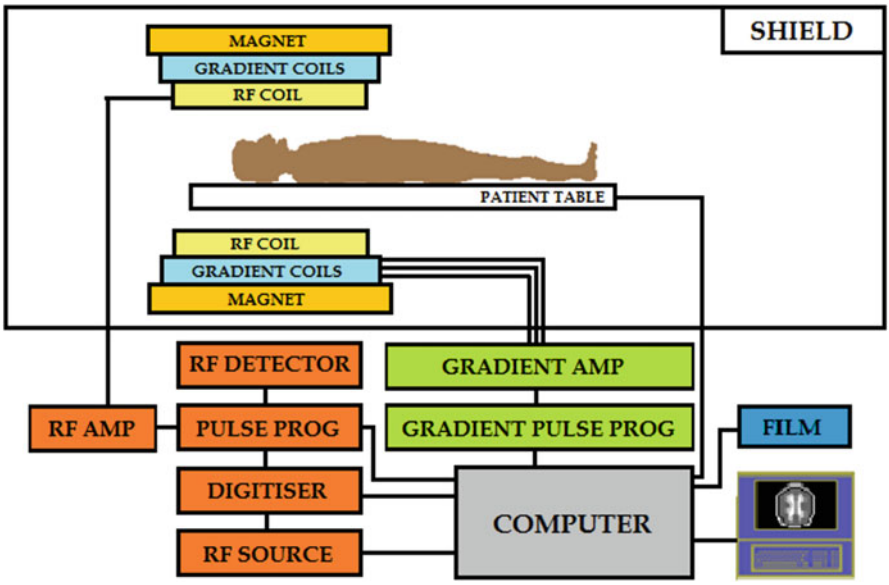

Fig. 6.14 Block diagram of a basic MRI hardware

6.4.4 *K*-Space and Image Formation

In general, the symbol "*K*" or "*k*" stands for momentum of a quantum particle or wave. It is conjugated to the real space denoted by *X* or *x*. On the other side, frequency (*n*) has inverse of time (*t*) dimension. A well-known technique in mathematics is the Fourier transformation that translates *k* to *x* or *n* to *t*. Thus, MRI data in space *X* can be saved in the *k*-space. There are several reviews available till now over

the techniques to fill points in *k*-space. The *k*-space can then be easily transformed into an image of high-contrast through a Fourier transform technique applied.

6.4.5 Pulse Sequence

At last, it is pertinent to just mention that the pulse sequence generally shows the timing of RF pulses and gradients. It determines the type of image as PD (proton density), *T*2-weighted, and *T*1-weighted to help in gathering better clinical insights on the nature of cells in human and other bodies.

6.5 Computed Tomography

Computed tomography (CT) is a widely adopted imaging technology used to inspect internal morphological structure of human organs and in industrial applications with high precision. This makes the technology a reliable tool for noninvasive evaluation of structural defects in engineering field and detection of unwanted growth and its progression in living bodies (Hounsfield 1973; Webster 2010). We will restrict our discussion to basic principle of computed tomography, development of CT scanning technology, and its clinical application. CT scan is based on imaging with X-radiation, and it has made a revolutionary change in clinical diagnosis of tumors, bone structure and deformation study, and selection of radiotherapy doses in cancer treatment.

6.5.1 Basics of X-ray

German scientist Conrad Röntgen discovered a new type of radiation in the year 1895 while he was studying experimentally different phenomena inside gas discharge tubes. This radiation was able to penetrate opaque tissues and objects so that the inner structural image like bone or skeleton for human body can be obtained. This development dramatically changed the medical diagnosis procedure. Being previously unknown, the ray was named as X-ray.

X-ray generator has a X-ray tube comprising of cathode and anode (Fig. 6.15). Cathode generates the electron beam that is collected by the anode. During the travel, electrons collide with the target and as a result a small fraction of the energy is liberated as X-ray, while the major component is converted to heat. The generated X-radiation is collimated and allowed to fall on the target or subject through the collimator aperture.

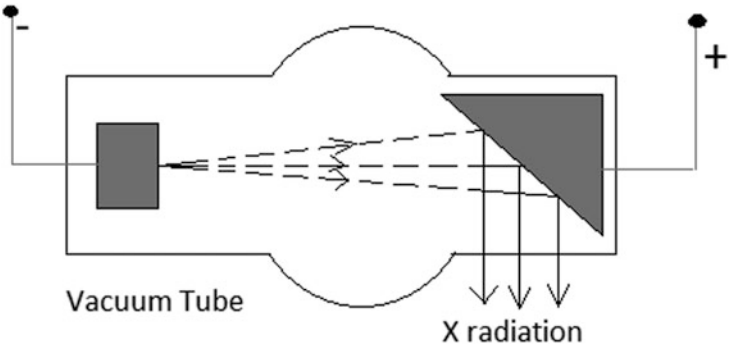

Fig. 6.15 X-ray production technique

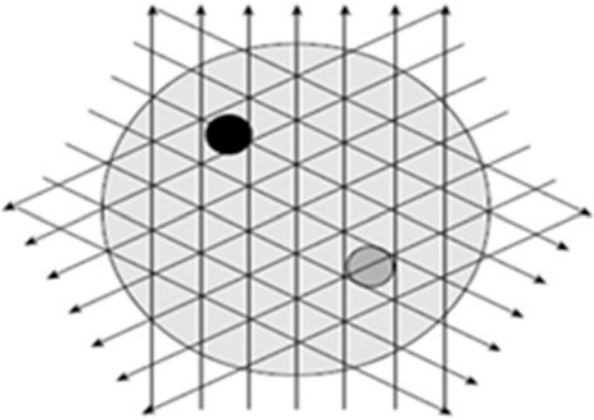

Fig. 6.16 Multidirectional X-ray transmission measurement through a slice of the subject

6.5.2 Diagnostic Application of Radiography

It is a well-known fact that different components of human body having different densities and thus possessing different absorption coefficients for X-ray. Therefore, an incident X-ray undergoes varying amounts of absorption in the organs while penetrating the human body. Thus, the outgoing radiation has spatial intensity variation as in the case of image. Multidirectional scanning through a slice is shown in Fig. 6.16. A suitable device that is capable to capture the intensity distribution can be employed to form the image of the section of the body. It is noticed that metallic foreign bodies, bones, and air cavities appear prominent in such imaging as the relative density of these sections is different from their neighboring tissues. But other organs of the body do not show much difference in intensity. Better image quality, clarity, and multidirectional view are possible to observe if special techniques like tomography are adopted.

6.5.3 Limitations of Radiography

There are some basic limitations of using conventional X-ray radiography (Hounsfield 1973; Barrett and Sweindell 1981). In general, two-dimensional X-ray plates have limited application in diagnosing 3D organs of the body as the dimensions of 3D objects are confusing in X-ray plate. Moreover, due to the limited dynamic range of the radiographic films, only larger intensity gradients are better visualized. So, the sections comprising soft tissues are difficult to estimate in radiography. Two closely spaced different organs with similar physical density can appear as a unit or the smaller organ may be lost from the image plate behind the larger one. Most of the body organs do not show much difference in intensity. Better image quality, clarity, and multidirectional view are possible to observe if special techniques like tomography are adopted.

6.6 Basic Principle of Computed Tomography

In CT scan, each slice of the subject is exposed in the radiation beam, which attenuates the radiation during its passage through the section. Governing factors of attenuation of the beam are incident intensity, composition, and density gradient of the medium through which the radiation is passed (Barrett and Sweindell 1981; Littleton 1976). This operation is performed over the entire section of interest through different angles, and the final image is reconstructed using specialized computer-based reconstruction algorithm (Cormack 1973).

In the earlier version of the CT scanners, the subject is scanned by a narrow X-ray beam and the detector is placed in the opposite side of the source beam to capture the transmitted radiation. If the subject is inhomogeneous and the beam is polychromatic, the intensity of the attenuated X-radiation is.

$$I = I_0 e^{-\sum_{i=1}^{n} \mu_1 X_1}$$

where I_0 is intensity of input beam, μ_i is the attenuation coefficient, and n stands for the scanned region with varying attenuation coefficients.

Different orientations of the beam source and the detector in a scan plane provide different attenuation coefficients in the transmission plane. The grayscale image is formed by assigning different brightness to each predefined range of the attenuation coefficient.

6.6.1 Image Viewing System

Formation and interpretation of the image are based on a derived parameter called CT number computed from the attenuation coefficients of the region which the beam

passes through during imaging. CT number, also known as *Hounsfield number* for any linear attenuation coefficient μ, is defined as.

$$\text{CT number} = 1000\frac{(\mu - \mu_W)}{\mu_W}$$

where μ_W stands for the linear attenuation coefficient of water. The normalized value of CT number in most CT units is restricted between -1000 for air and +1000 for bone (Cierniak 2011; Rao and Guha 2001).

Attenuation coefficients for different body tissues slightly differ from each other. The differential attenuation coefficient is thus highly correlated with the physical density. Hence, the image reconstructed as a result of computed tomography can be considered as the mapping of densities with respect to that of water. Typical CT numbers of various body tissues are as follows: fat–60, brain white matter—30, brain gray matter—38, blood—42, muscle—44, etc.

6.7 Components of CT Scanner

A typical CT scanner has the following components: gantry, X-ray source, X-ray detector, and data acquisition system and finally the computer and operator console. The synchronized operation of the components develops the required image information of clinical relevance. Brief description as given below of the physical components of CT scanner may be pertinent to understand its functioning. The scan room arrangements are shown in Fig. 6.17.

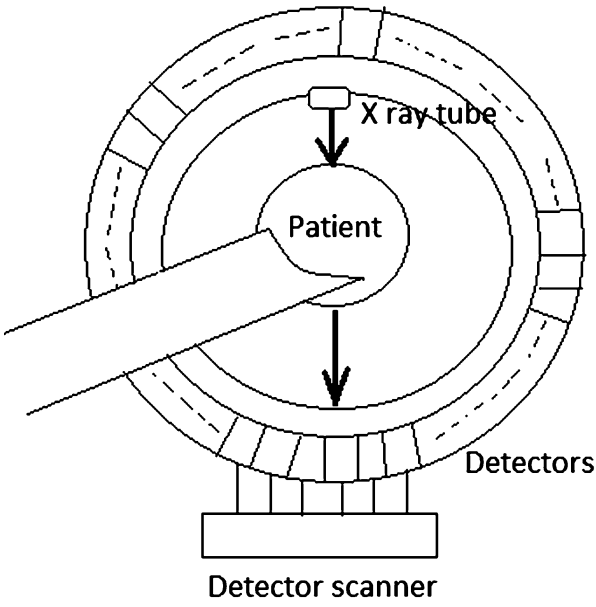

Fig. 6.17 Major components of scan room arrangement

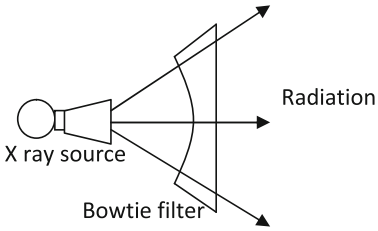

Fig. 6.18 X-ray source and bowtie filter

Gantry: It is the patient end component of the CT scanner, where the units like X-ray source and detector system are fitted along the periphery of the ring-type unit (Fig. 6.17). The patient table is mounted at the aperture of the gantry where the patient is allowed to lie down during scanning. The mechanical arrangement is provided to rotate the X-ray source and detector system such that the radiation source can scan the section of interest and the related output radiation be captured by the detectors.

X-ray source: The technique for generating X-radiation is introduced in Sect. 6.5. The collimated radiation is allowed to fall on the section of interest of the body with full alignment with the detectors. The section of the beam away from the detectors' scope is restricted by the collimator. The low-energy beam (soft X-ray, having low frequency) that cannot penetrate the body is filtered by the grid. Further filtration of the beam is performed to reduce the radiation exposure of the patient and to minimize beam hardening issues as well. This, in turn, improves the CT image quality. X-ray filter is designed to provide uniform radiation to cross section of the body. As human body has circular cross section and the thickness reduces gradually toward the periphery, filters are designed to reduce X-ray intensity toward the periphery with respect to the central area. Such filter is shown in Fig. 6.18, which is named as bowtie filter due to its specific shape.

6.7.1 X-Ray Detector and Data Acquisition System

The emerging radiation flux is absorbed in the detector array with rapid response time. The detector system rotates synchronously with the source and converts the absorbed beam into a proportional detector signal (Webster 2006). The resolution of the image mainly depends on data acquisition rate, detector geometry, and the size of the focal spot of the source. Mainly three types of detectors are used in CT scanners:

Scintillation detector: Hounsfield originally used a detector made up of sodium iodide (NaI) scintillation crystal combined with a photomultiplier tube (PMT). The scintillation crystal absorbs the transmitted X-ray beam, which is converted into light photons. PMT receives the visible light through a quartz or glass window covering the surface of photocathode. It, in turn, emits electron proportional to the light quanta. The electrons are multiplied in the series of metal channel dynode. Finally, the anode at the end of the dynode series generates current proportional to the absorbed radiation. The schematic operation is shown in Fig. 6.19.

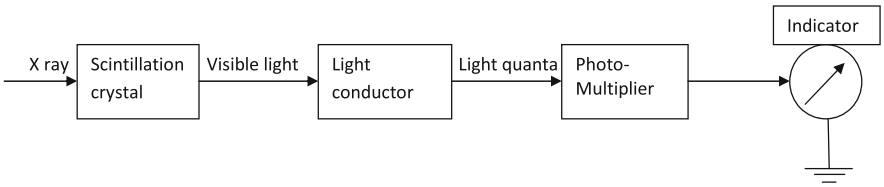

Fig. 6.19 Scintillation crystal and photomultiplier

Xenon gas ionization detector: In these detectors, the X-ray is allowed to pass through a chamber filled with inert gas like xenon. The energy of the incident radiation ionizes the gas. Resulting electrons are collected by a set of electrodes. The current flowing through the output circuit is proportional to the incident radiation. In order to increase the interaction between the gas and the incident radiation and thus to increase the output signal level, operating pressure in the xenon chamber is kept high.

Scintillare: It contains scintillation and photodiodes in order to collect the beam. The scintillation detector is small dimension such that it permits good resolution. The optical signal from the scintillation detector is allowed to fall on the photodiode through optical fiber. Photodiode generates the electrical signal, which is sent to the computer for data reconstruction using array processors.

Computer and operator console: The attenuation of the source radiation is detected by the X-ray detector and data acquisition system, and the resulting electrical signal is received by the computer, which digitally reconstructs the image using the projections from all slices. The overall control of operation like start, progress, and end of scan is also preserved by the operator's console. Patient information and other clinical information are also handled in this section.

6.8 Reconstruction of CT Image

The scanning data are required to be processed using specialized mathematical algorithms to reconstruct the image of the scanned section (Ledley et al. 1974; Hendee and Ritenour 2002). In the iterative mode of data reconstruction, one initial pattern of the image is guessed and the reconstructed data are mathematically compared with the guess for minimum deviation. In this mode, the manner of variation of the model each iterative step is also noted along with the voxel-based X-ray attenuation coefficients. The deviation between the model and the measured pattern is minimized by modifying the pixel intensity values along the path of the beam for each iterative step. The intensity pattern is a complicated function of X-ray direction, absorption coefficient, detector location, and projection angle (Goldman 2007). This intensity function is represented by *radon transform* of the attenuation coefficients over the entire scan plane. Explicit mathematical formulation is required for reconstruction of the image by inversion of the *radon transformation*. A point in image space is represented by a sinusoidal pattern in a plane created by the projection angle and the detector number.

6.9 Evolution of CT Scanning Technology

Hounsfield first incorporated a computer with X-ray imaging technology for scanning the brain in 1971; however, tomographic techniques were in use since the 1930s. Because of the ability to demonstrate anatomical information with final detail, computer-assisted tomography (CAT) attracts the interest of the clinicians. With the development of data acquisition hardware electronics and data processing technology, gradually the scan time and the information quality were enhanced with the newer generation of CT system. Depending upon this, the technology is mainly divided into four generations:

6.9.1 First-Generation CT (Translate–Rotate Mode)

In first-generation CT system, pencil-like narrow X-radiation beam was used with a single detector mechanically linked to each other. The source–detector system translates along the patient to cover his/her full width and then is rotated by 1°. Each translation took about 4–5 s. Thus, the entire scan is completed with the data captured from 180° of rotation. The average scan time is 25–30 min using this technique. A later design consists of a detector pair to handle two slices at the same time. Hounsfield's first brain scanning system uses a water bath where the patient's head covered with an elastic membrane is place such that the X-radiation passes through the water to reduce the dynamic range of radiation. However, this is not suitable for whole-body scanning. Figure 6.20 shows the imaging technique of first-generation CT scanners.

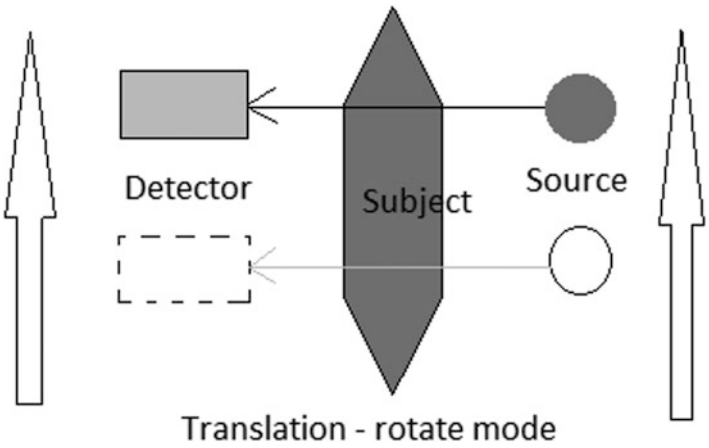

Fig. 6.20 Translate–rotate mode of first-generation CT scanning

6.9.2 Second-Generation CT (Multidetector Translate–Rotate Mode)

Second-generation CT was the outcome of the research toward minimization of the scan time. For that, additional detectors were used in the form of an array in the scan plane and a narrow fan beam of X-ray replaced the pencil beam. Because of the presence of detector array, the rotational angle is increased up to 20°–30°, which considerably reduced the scan time. As human is capable to hold the breath for at least 10 s, it was possible to capture chest CT image using this variant of CT scanner; however, the motion of heart causes noise in chest imaging. Figure 6.21 represents the scanning technique of second-generation CT scanners. This generation of CT scanners introduced table movement and laser-based slice indication and reconstruction technique based on Fourier transformation.

6.9.3 Third-Generation CT (Rotate–Rotate Mode)

Here, the rotate–rotate mode of scanning is adopted as now the gantry is equipped with few hundreds of detectors covering the total width of patient synchronized with a fan beam of X-ray (Fig. 6.22). With a very large data set in the output side, this technique requires efficient computing facilities. The scan time is reduced round 2 s in this orientation. This type of scanner is still in use in most of the clinical applications. However, this rotate–rotate mode generates the ring artifact in the

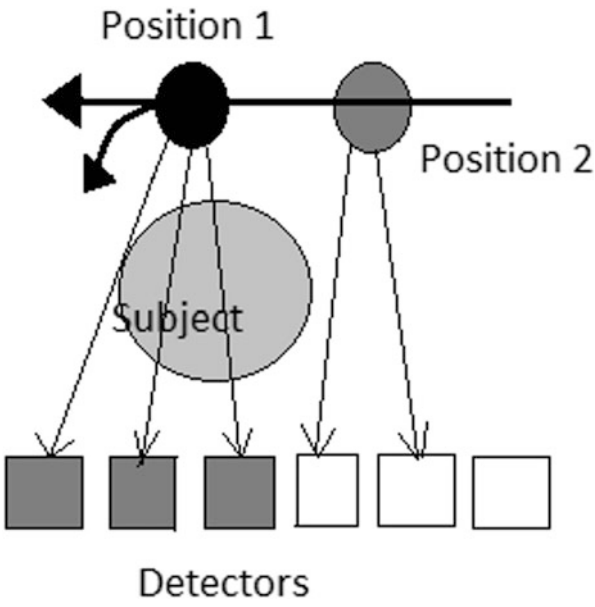

Fig. 6.21 Translate–rotate mode with multidetector for second-generation CT scanning

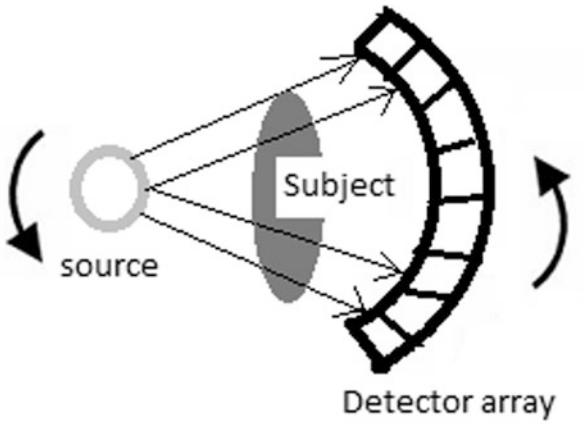

Fig. 6.22 Rotate–rotate mode of third-generation CT scanning

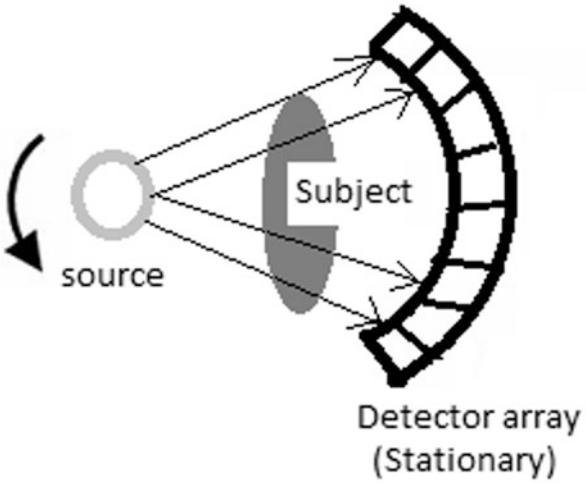

Fig. 6.23 Fixed–rotate mode of third-generation CT scanning

reconstructed image, which was minimized but not completely eliminated using xenon detectors.

6.9.4 Fourth-Generation CT (Fixed–Rotate)

The fourth-generation CT is developed specially to eliminate the ring artifact. In this case, more numbers of detectors up to few thousands are fixed on the gantry and a fan beam is used as X-ray source. Fixed detectors receive the attenuated radiation from the rotating source along the ring as shown in Fig. 6.23. Here, each detector is exposed with a complete fan beam as the beam passes across each detector.

Further developments including oscillating ring of detectors, steerable electron beams, 2D detector arrays, and helical data acquisition are sometimes given generation numbers, but not applicable in regular manner.

6.9.5 Electron Beam CT (Fixed–Fixed)

This provides a relatively new technology especially rapid cardiac imaging for screen coronary artery disease where the scan time is further reduced to synchronize the system with cardiac dynamics. Fixed set of detectors system with movable source is used, which encircles the patient (Goldman 2007). Source used here is an electron gun instead of conventional X-ray. The source is rotated electronically around the subject in EBCT.

6.9.6 Helical CT

In helical type, CT scanning patient faces a translation movement along the gantry and the X-ray source moves along a helical path around the patient. This technology was introduced in 1989 and adopted throughout for CT scanning (Lee et al. 2007). The helical motion of the tube is supported by a sliding contact-type arrangement such as slip ring. With this revolutionary up-gradation, the data acquisition time is reduced significantly. This results in a 3D image data of the slice per rotation of the tube, which requires efficient reconstruction and interpolation to estimate the actual image.

6.10 Clinical Application of CT Scan Image

As mentioned in the earlier sections, computed tomography not only captures images of different internal structures but also can differentiate the organs like lung, liver, and colon from other internal organs and fat. CT imaging has significant application in identifying large masses like tumors and metastatic growth at different volumes of human torso (Bar-Shalom et al. 2003). CT imaging and reconstruction procedures can also point out toward the shape, size, volume, and location of the growth. Besides, CT images can reveal brain hemorrhage and clot, blood vessel defects, and enlargement of different organs. Recent advances in image processing technology enable us to develop assistive diagnostic technologies for automatic detection of tumors or unnatural growths from the CT image. The general steps of CT image processing are given in Fig. 6.24.

To reduce the risk of radioactive exposure, radiation dose is reduced within a certain limit, which degrades the quality of image. The subject movement, respiration, etc., also introduce noise in the image. Image smoothing and enhancement retrieve the blurred image by filtering. Gaussian filter, bilateral filter, Gabor filter, Weiner filter, threshold-based enhancement, etc., are the most popular techniques for

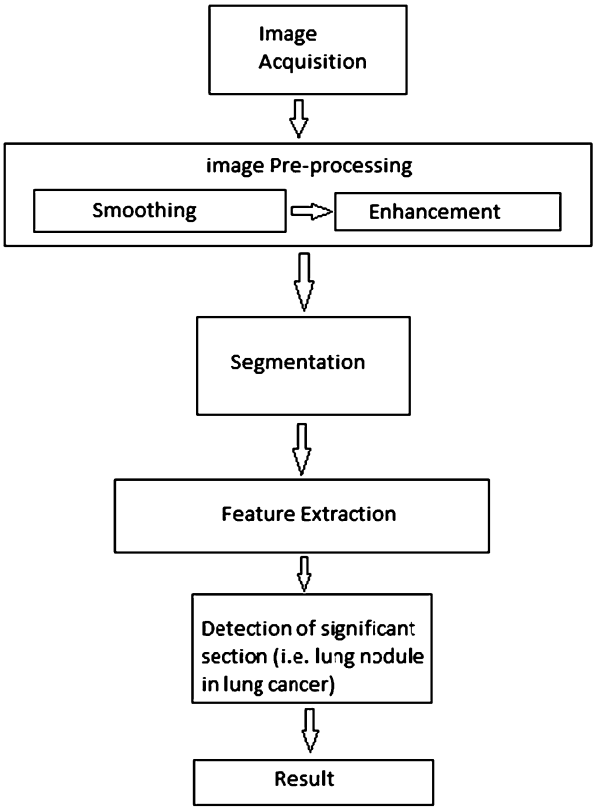

Fig. 6.24 Steps for CT image analysis

image denoising (Bar-Shalom et al. 2003). Segmentation is the technique to partition the image into a number of sections to isolate the tissues of organs of interest like lung and colon from the adjacent mass. It is generally done by grouping the pixels (or voxels) of similar intensity of predefined range and isolating them from the other pixels (or voxels) to form the object of interest. Automated classification of segmented image is done by classifiers based on advanced mathematical techniques such as fuzzy logic, artificial neural network, and support vector machine. Actually, pixel-based input image information is too large to be dealt with by the classifier due to computational complexity. A smarter approach is to extract relevant features from the image and design a classifier. For example, dimensional features of lung nodules can be used for staging the tumor. Also, the gradual variation in volume of the tumors in malignancy is helpful to select the radiotherapy doses for a patient.

Use of CT is also prevalent in orthopedic studyfor bony structures analysis and bone density study, imaging of complex joints like the spine, shoulder, or hip for fracture healing, deformation study, etc.

6.11 PET Scan

In the physicist's world, particles and their antiparticles form a fascinating view of how matter is made of. As we move from the molecule to the atom and then in the central tiny-sized nucleus surrounded by the revolving electrons, we see a totally different and interesting behavior of the subatomic particles. Soon after the firm foundation of quantum mechanics, Paul Dirac, the British Nobel winner physicist, predicted the existence of antiparticles theoretically in 1928, and their existence was confirmed experimentally. The particle known as *positron* is basically anti-electron or the antiparticle or the antimatter counterpart of the electron. The *positron* has an electric charge of +1 e, a spin of 1/2 (the same as that of an electron), and has the same mass as an electron. Carl Anderson, the American Physicist, discovered positron. Thereafter, many other antiparticles like antiproton and antineutron were successfully discovered.

In the year 1896, Henry Becquerel, a French Physicist, discovered *radioactivity* that relates to the emission of alpha, beta, and gamma rays from certain substances or nuclei like uranium. Madame Curie discovered radium, another well-known radioactive element. Later, alpha rays were identified as helium nucleus, beta (β^-) as electron, and gamma as photons. Positron emission is basically a beta-plus decay (β^+ decay), another form of radioactive decay. Here, a proton inside a radionuclide nucleus is converted into a neutron while releasing a positron and an electron neutrino (ν_e). Positron emission is mediated by the *weak force*, one of the four fundamental forces in nature.

6.12 PET Scan: Basic Principle

A PET scan is an imaging technique that can help us to know how well the tissues and organs in our body are working, especially metabolism, oxygen use, and blood flow to the organs. PET stands for positron emission tomography (Strunk et al. 2018). Fig. 6.25 shows what a PET scan machine looks like.

This type of scan requires that a small amount of radioactive material be delivered into the patient's bloodstream through an intravenous injection. This radioactive material is known as a tracer. Once the tracer has time to work through the body, the patient is taken back to the scanning machine to have the procedure done. The PET scan is a gigantic machine containing a tunnel as in MRI. The patient has to lie on a hard table that can move his or her body into the tunnel. Once the body enters the tunnel, the PET reads signals sent from the tracer. The machine converts these signals into 3D pictures, which are further interpreted by a specialist (radiologist). The tracer when injected into the body is active only for the duration of 2–10 h. The radiation eventually loses its potency and leaves the body normally through urine. Patients are advised to drink plenty of water after the procedure to help speed up this process.

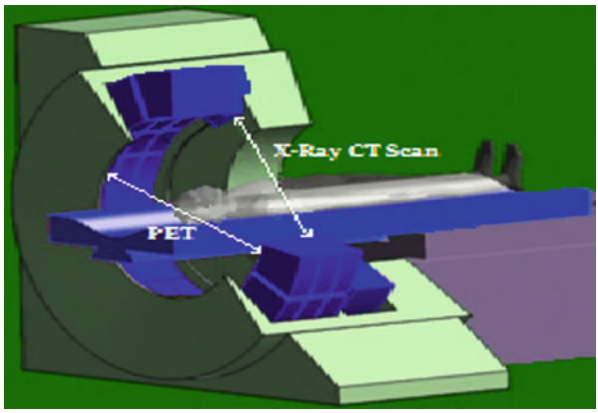

Fig. 6.25 PET scanner: a marvel realized by the synergy of different imaging methods

6.12.1 PET Scan Utilities

PET scans can directly show how our internal organs are working and indicate the presence of any abnormality. So, it is a very effective test to look for the diseases and functionality of the organs. It helps in detecting abnormalities or lumps or masses inside the body, checking whether cancer treatments have been effective or the disease has recurred, any disorder in brain such as tumors, seizures and Alzheimer's disease, heart disease, weakened heart muscles, blockages and decreased blood flow, etc.

6.12.2 Early Detection of Malignant Tumors/Cancers

PET scan today helps doctors across the globe to execute accurate diagnoses of patients before a disease spreads irreversibly. It can further help to monitor continuously the recovery from surgical operations. During cancer treatment, oncologists use PET scans to identify any potential tumor inside the body. Later, they can see the progress of their patients with treatments like radiotherapy or chemotherapy. The detailed images obtained with the help of PET can guide the doctors in assessing the condition of the patients properly. It can help also to stop inefficient treatments, replacing usual surgery with radiotherapy or the future course of actions to be taken.

Beta-plus radioelements, emitters of positive electrons or positrons, are used as the radioactive tracers in this machine. It is a common fact that positrons annihilate by emitting two back-to-back gamma rays or photons within a short time. Thereafter, we need to detect simultaneously these gamma or photon pair so as to locate the specific zone of emission close to the fixation of the radioactive tracer. With this detection of a large number of photon pairs, we can map the points in our cells containing radiotracers in order to screen the hot spots with greater resolution. In this context, we use a term known as *scintigraphy*. It is a technique using the scintillation counter or similar detectors with a radioactive tracer to produce n very high-quality

image of a body organ or a record of its functioning. Normally, isotopes like iodine 131 (^{131}I) or technetium 99 (^{99}Tc) are commonly used in scintigraphy. Radioactive iodine 131 is generally used for medical purposes. If a small dose of iodine 131 is swallowed, it gets absorbed into the bloodstream of the gastrointestinal (GI) tract and concentrated from the blood by the thyroid gland, where it begins destroying the gland's cells. On the other hand, the isotope technetium 99 can be easily detected in the body by medical techniques. The reason is that it emits 140.5 keV gamma rays, which are similar to the conventional X-rays. Further, its half-life for gamma or photon radioactive emission is about 6 h, which means half of the initial number of radioactive atoms decays in about 6 h. Generally, the positron emitters are elements like oxygen, carbon, and nitrogen that are abundantly available in the body. Further, halogens like fluorine 18 or bromine 76 can easily be attached to other molecules. This means that chemicals involved in the human metabolism can be attached to different radioactive elements and made to flow inside the body. For example, the way human tissue absorbs glucose can be properly mapped after an injection of a compound FDG (fluorodeoxyglucose), which contains radioactive element fluorine 18 (^{18}F). The absorption of glucose can monitor a person's health as it can reveal important information on how different tissues work in our body organs like brain, heart, or any malignant tumor.

It is a commonly known fact that water molecules form a major constituent of the human body. The molecular structure of water is simple with two hydrogen atoms covalently bonded to a single oxygen atom. The water molecule can be marked with oxygen 15 and can be used to follow the path of blood flow inside the brain. Thus, it can provide a greater understanding of the way it works. These explorations have paved the way for new insights into neurology, psychology, linguistics, and the cognitive sciences. Unfortunately, beta-positive isotopes do not exist in nature and must be created in the laboratory. It is now an established fact that the half-lives of these artificial positron emitters are very short. Oxygen 15 has a period of 2 min, while the amount of fluorine 18 halves in just under 2 h. These isotopes must therefore be inserted into the body as soon as possible after they are created in the laboratory of the hospitals having a cyclotron facility or other mini-accelerators. Another important fact is that FDG is the most widely used one among all the chemicals marked with positron emitters. It has a comparatively long half-life, and so, it can be easily transported from its production site to diagnostic centers in the close-by area. Reportedly, FDG has been used in PET scan for the full-body scan performed in clinical oncology to determine the spread of cancer (Oehr et al. 2004).

6.13 Conclusion

MRI is safe as far as the latest study reports suggest except for the persons who carry non-MRI-compatible implants and metallic components near some vital organs inside the body. It is a common observation that the much-needed MRI is sometimes avoided by the people as the small imaging space leads to a claustrophobic feeling and therefore nervousness. Further, recent studies have established that patients with

kidney problems may need extra monitoring during MRI scan. Anyway, MRI is undoubtedly a better imaging technique having no radiation exposure but high-quality resolution although it is a relatively time-taking process.

Computed tomography has a significant position in the history of clinical diagnostic imaging. In terms of engineering knowledge and its application, it achieves a superior height by collectively applying X-ray imaging, use of rotary radiation detector arrays, mathematical methods for reconstruction of the image, and computer capabilities as a whole to produce a novel way of noninvasive analysis of internal organs of human body. Actually, CT became exceptionally useful because of its ability to generate better contrast of image of adjacent but different mass of tissues of different organs, which are neither readily accessible nor observable by other imaging techniques. The main advantages of computed tomography are most detailed and informative among all imaging techniques (refer to Fig. 6.26), the process is rapid and painless, clear, and specific information about the morphological structure of the growth based on which a reliable clinical decision can be suggested, and large portion of the subject can be viewed at the same time. But like any other radiation type imaging, computed tomography has also some disadvantages: Risks due to higher dose of radiation are greater than other imaging types and which is greater for children, injection of a contrast medium (dye) can cause kidney problems, and iodine-enriched contrast dye may cause allergic reaction in patients. Cancer detection and preparation of treatment protocol have become easier with the development of CT images. Moreover, the effectiveness of treatment can also be studied by consulting the CT images successively captured within the duration of the treatment.

The latest technological advance in the field of medical imaging for cancer screening has been achieved by combining the two methods of "*computed tomography*" and "*positron emission tomography.*" This composite method being much informative helps in diagnosis otherwise difficult with other single imaging techniques like CT or MRI. Thus, an X-ray scanner is also attached to the PET cameras. The images produced by scanner are very precise from an anatomical point of view. But it cannot provide much information on cell metabolism like the changes within the substances they are made of. In contrast, PET images are sensitive to the metabolism and so functional in projecting more information. But these images suffer from the qualities of sharpness and precision from an anatomical point of view. So, the CT images can be combined with the functional images from PET scan in a hybrid device. The combination of these two images can precisely locate an injury or malfunction. This helps optimize a protocol during radiotherapy. So, it makes an operation more efficient, avoiding unnecessary surgical procedures, or reduces the use of invasive procedures such as biopsies. As the CT scanner and the PET camera are side by side and the patient does not need any movement move between the two tests, the merging of two images is of excellent quality. Due to the high speed of the scan usually less than 30 min, the results can be processed quickly compared to a day in the past days. Thus, it helps in drawing a more reliable and accurate diagnosis for the sick patients and in cases of suspected cancer. Finally, the

distinguishing features of the three different imaging methods are summarized in the following table (Ref. Thedens 2013).

Modality	Approximate resolution	Source of energy	Image contrast of the source	Advantages	Limitations
CT	0.2–1.0 mm	X-ray	Tissue density	Fast, high resolution, and 3D reconstruction	Poor soft tissue contrast, radiation dose
MRI	0.3–1.0 mm	Radiofrequency	Multiple	Soft tissue contrast, multiple contrast methods	Scan times, metal, patient comfort
PET	4–7 mm	Positrons/ gamma rays	Tissue biochemistry	Tissue function information	Low resolution, radioactive elements

References

Barrett HH, Sweindell W (1981) Radiological imaging-the theory of image formation, detection, and processing, vol 2. Academic Press, New York

Bar-Shalom R et al (2003) Clinical performance of PET/CT in evaluation of cancer: additional value for diagnostic imaging and patient management. J Nucl Med 44(8):1200–1209

Brown MA, Semelka RC (2003) MRI: basic principles and application, 3rd edn. Wiley – Liss, Hoboken, NJ

Cierniak R (2011) X-ray computed tomography in biomedical engineering. Springer-Verlag London Limited, London

Cormack AM (1973) Reconstruction of densities from their projections, with applications in radiological physics. Phys Med Biol 18(2):195–207

Goldman LW (2007) Principles of CT and CT technology. 35:115–128

Hendee WR, Ritenour ER (2002) Medical imaging physics, 4th edn. Wiley-Liss, Inc., New York

Hounsfield GN (1973) Computerized transverse axial scanning (tomography), part 1: description of system. Br J Radiol 46:1016–1022

Liang Z-P, Lauterbur PC (2000) Principles of magnetic resonance imaging: a signal processing perspective. SPIE Optical Engineering Press, New York

Ledley RS, DiChiro G, Luessenhop AJ, Twigg HL (1974) Computerized transaxial x-ray tomography of the human body. Science 186:207–221

Lee KS, Yi CA, Jeong SY et al (2007) Solid or partly solid solitary pulmonary nodules: their characterization using contrast wash-in and morphologic features at helical CT. Chest 131:1516–1525

Littleton JT (1976) Tomography: physical principles and clinical applications. Williams and Wilkins

Oehr P, Biersak HJ, Coleman RE (2004) PET and PET-CT in oncology. Springer-Verlag, Germany

Rao CR, Guha SK (2001) Principles of medical electronics and biomedical instrumentation. Universities Press, Hyderabad

Strunk A., Gazdovich J., Redouté O., Reverte J. M., Shelley S. & Todorova V., 2018 Model PET scan activity. The physics teacher 56, 278https://doi.org/10.1119/1.5033868

Thedens DR (2013) PhD and International Center for Postgraduate Medical Education. www.icpme.us

Webster JG (2006) Encyclopedia of medical devices and instrumentation, vol 2, 2nd edn. John Wiley & Sons, Inc., Hoboken, NJ

Webster JG (2010) Medical instrumentation application and design, 4th edn. John Wiley & Sons, Inc., Hoboken, NJ